

NUMERICAL AND EXPERIMENTAL INVESTIGATIONS IN ULTRASONIC HEAVY WIRE BONDING

Reinhard Schemmel, Tobias Hemsel, and Walter Sextro¹

¹ University of Paderborn, Chair of Dynamics and Mechatronics
Warburger Str. 100, 33098 Paderborn, Germany
reinhard.schemmel@upb.de, tobias.hemsel@upb.de, walter.sexstro@upb.de

Key words: wire bonding, time variant frictional contact, wear, substructure, ultrasound, model order reduction

Abstract. Ultrasonic wedge/wedge-wire bonding is used to connect electrical terminals of semiconductor modules in power electronics. The wire is clamped with a tool by a normal force and ultrasonic vibration is transmitted through the wire into the interface between wire and substrate. Due to frictional processes contaminations like oxide layers are removed from the contact zone and the surface roughness is reduced, thus the real contact area is increased. In the next step of bond formation, thermomechanical forces create micro-junctions between the wire and substrate and the bond strength increases.

The bond parameters like the bond normal force, the ultrasonic vibration amplitude and the geometry of the clamping tool show a high influence on the strength and reliability of the wire bond and need to be investigated in detail. Therefore, in this contribution the dynamical behaviour of the ultrasonic system, the wire and the substrate are modeled in form of substructures, which are connected by the friction contacts between tool and wire and between wire and substrate. Approaches for modelling the time variant contact behaviour, the substrate dynamics, and the model order reduction for a time efficient simulation are described to simulate the full bonding process.

1 Introduction

Ultrasonic wedge/wedge wire bonding is a well known technology which is industrially used to connect electrical terminals of semiconductor modules in power electronics. Aluminum wire is preferably used in heavy wire applications because of its robust bonding behaviour and low cost. The challenges due to rising electrical power in high power applications, such as wind turbines, electrical vehicles or solar modules are higher thermal and mechanical stress of the junctions. The limits of aluminum wire bonds can be overcome by copper wire bonds because of their significantly higher electrical and thermal conductivity and mechanical stability. Because of the different material properties, the bonding parameters in copper wire bonding differ significantly from those of aluminum wire bonding. The ultrasonic power and the normal bonding forces are about 2 to 3 times higher. Also, the copper wire bonding process reacts more sensitive to parameter changes and wear of the ultrasonic tool (wedge) is increased. This

makes manufacturing of reliable copper bond connections challenging, [Chauhan et al. 2014], [Eichwald et al. 2016] and [Schemmel et al. 2018]. To understand the complex process of bond formation and for the optimization of the bond parameters, detailed modelling of the highly dynamical and non linear mechanical contact is essential.

In this contribution, first a description of the bond process and the ultrasonic system is presented. The contact behaviour between wedge and wire is modeled for micro wear simulations and geometry optimizations to increase the transmittable tangential force. A time variant contact model and a discretized micro-slip model for the interface between wire and substrate for simulations of the bond formation are discussed. Substrate dynamics play an important role in ultrasonic wire bonding, especially when bonding on supple substrates. Therefore, a method for creating a state space model for the substrate-substructure and a model order reduction, based on the "Hankel Singular Values", are presented.

2 Description of the wire bonding system and the bond process

The bonding system consists of an ultrasonic transducer which is fixed in the bonding machine by a clamp, **Figure 1**. The transducer is excited by an oscillating voltage U which is transformed to a mechanical oscillation by the piezoelectric ceramics. The transducer is operated at the resonance frequency of a longitudinal vibration mode. Typical bond frequencies of the transducers for heavy wire bonding lie in the range of 40 to 100 kHz. The oscillation amplitude x_T at the tip of the transducer is used to excite a bending mode of the wedge. The wedge is attached to the transducer by a bolt and transmits the oscillation of the wedge to the wire. The tip of the wedge for heavy wire bonding has the shape of a v-groove to clamp the wire by the bond normal force F_{bn} . The wedge-tip is typically made of tungsten carbide or titanium carbide [Long et al. 2017].

The bond process is divided into 4 phases. In the first phase ("Pre-Deformation Phase") a static "Touchdown Force" F_{TD} is applied and the wire is clamped between the wedge and the substrate at the bond position. In the next phase ("Cleaning Phase"), the ultrasonic vibration x_w and the bond normal force F_{bn} , which can differ from F_{TD} , are applied to the wire, that starts to move on the substrate. Due to friction processes in the interface, contaminations like oxide layers are removed and the surface roughness is reduced. Thus the real contact area of metal-metal contact is increased [Althoff et al. 2015]. In the third phase ("Deformation Phase"), thermomechanical forces and additional shear stress in the wire due to the ultrasonic vibration lead to high plastic deformation of the wire, even though the normal force F_{bn} is not increased significantly; the effect of high deformation under influence of ultrasonic vibration is known as the "Ultrasonic Softening Effect", [Daud et al. 2007]. In the Deformation Phase, first micro-junctions are build and the relative motion between wire and substrate is reduced to partial micro-slip. In the last phase ("Interdiffusion Phase"), the material bond between the wire and substrate develops. A material flow between wire and substrate can be seen, which is activated by the ultrasonic induced stress in the interface [Sbeiti 2013].

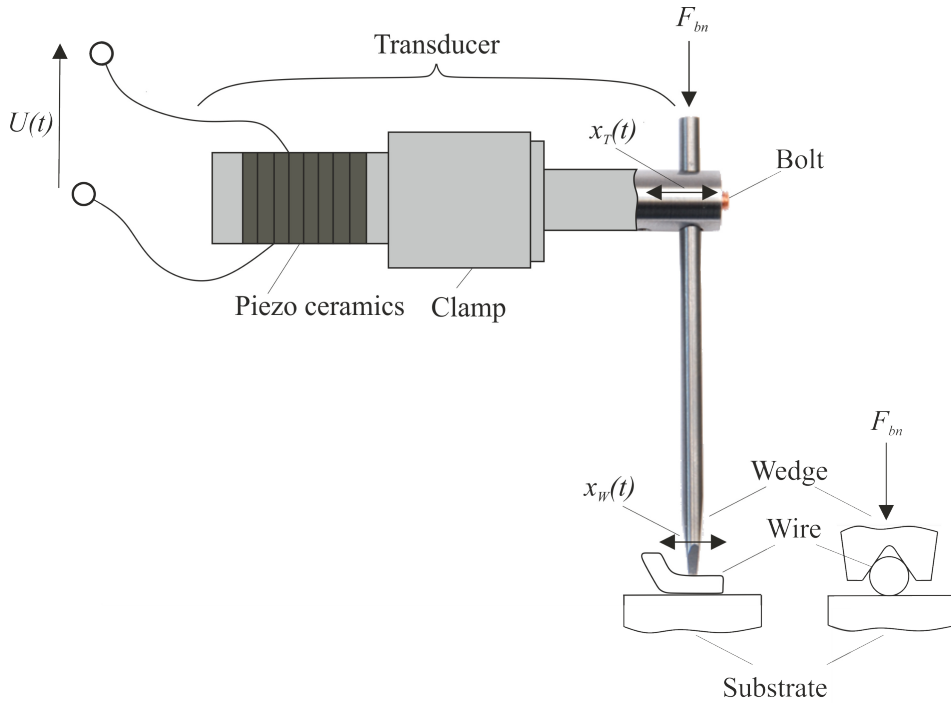


Figure 1: Bonding system for heavy wire bonding, consisting of the ultrasonic transducer, driven by the oscillating voltage $U(t)$, and the wedge, clamping the wire by the bond normal force F_{bn} . The wedge is excited to a bending oscillation by the transducer amplitude $x_T(t)$ and the wire is excited by the wedge amplitude $x_W(t)$.

3 Modelling the contact between wedge and wire

In ultrasonic wire bonding, the contact between wedge and wire fulfills different basic requirements, [Althoff et al. 2016]. First, the contact is crucial for the transmission of the tool tip oscillation x_W to the interface between wire and substrate. On the other hand, slippage between wedge and wire protects the already bonded wire from damage when ultrasonic vibration is still applied during the interdiffusion phase. Finally, to guarantee a stable process over hundreds of thousands of bonds for a cost efficient production of microelectronic products, wear processes in the v-groove and their influence on the bond formation have to be considered.

An appropriate way for geometry optimizations of the wedge geometry is to use the finite element simulation under the consideration of plastic deformation of the wire and the nonlinear frictional contact between wedge and wire, [Althoff et al. 2016], [Eichwald et al. 2017]. The main parameter of the geometry of the v-groove is the angle α , **Figure 2**. The angle α influences the clamping force F_{wn} by a force enlargement of the bond normal force F_{bn} and thus the maximum tangential force, that can be transmitted to the wire. Simulation results show, that with decreasing tool opening angle α , the ratio $\frac{F_{wn}}{F_{bn}}$ and the transmittable tangential force increase.

Besides the angle α , the shape of the v-groove has an important influence on the bonding results; e. g. additional ridges can reduce the slippage between tool and wire and increase the lifetime of the tool, [Xu et al. 2015]. A change of the tool-tip geometry due to wear processes

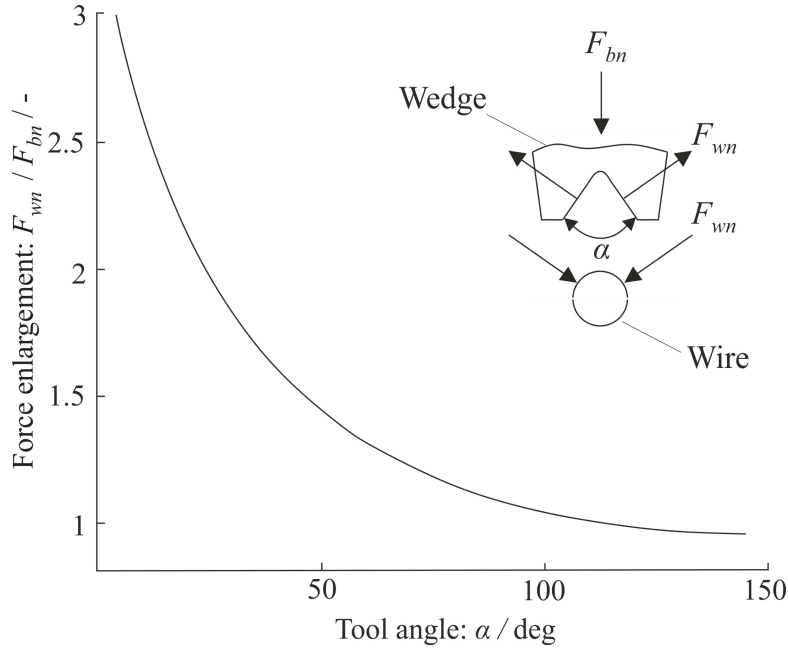


Figure 2: Analysis on the influence of different angles α of the v-groove on the clamping force F_{wn} , [Althoff et al. 2016].

leads to varying bonding results over the tool-lifetime. In [Eichwald et al. 2016], a finite element model is presented to simulate the wear in the v-groove based on Fleischer's wear law:

$$\dot{V} = \frac{1}{e_f^*} P_f \quad (1)$$

In Eq. 1, P_f is the frictional power and e_f^* the frictional energy density as a characteristic parameter for the wear of the frictional contact. Fleischer's law is used for calculating the volume loss in the v-groove by simulating the tangential excitation and the resulting micro-slip in the contact between wedge and wire. From simulation results of micro wear for different angles α follows, that an angle α of 90° is beneficial for a constant and uniform volume loss in the v-groove. This leads to a more stable and robust bond process over hundreds of thousands of bonds. In Figure 3, the unworn geometry of the v-groove of a tool for a $500 \mu\text{m}$ copper wire bond process and the worn geometry after ≈ 100000 bonds can be seen. The worn geometry of the v-groove leads to a different deformation behaviour; the width of the bond increases and a less smooth contour of the bond compared to the unworn geometry of the v-groove is observed, [Broekelmann et al. 2016]. A highly deformed wire as a result of the worn v-groove can reduce the reliability of the bond connection because of stress induced failure mechanisms like so called "heel cracks", [Celnikier et al. 2011]. When using the worn wedge geometry in finite element simulations, the influence of the geometry change of the v-groove on the normal contact pressure distribution between wire and substrate can be seen; for a given bond force F_{bn} , the worn wedge geometry leads to a larger interface area with increased width and the mean normal contact pressure is less, compared to the initial geometry. Additionally, the geometry change of the v-groove leads to a different clamping force F_{wn} , thus the transmittable tangential

force changes.

In summary, different aspects have to be considered for the tool design in heavy wire bonding. For optimizations of the tool geometry, finite element simulations should be used, analyzing the micro-wear processes and the transmittable tangential force in the contact between tool and wire. The geometry of the unworn geometry should be designed for a high transmittable tangential force. This can be achieved either by changing the angle α of the v-groove or by modifying the geometry of the v-groove with additional ridges clamping the wire. From simulation results of micro wear in the contact between tool and wire follows, that an angle α of 90° is beneficial for a constant and uniform volume loss in the v-groove. This leads to a more stable and robust bond process over hundreds of thousands of bonds. Both goals, a high transmittable tangential force and less/uniform micro wear in the contact, can not be achieved with the same angle α leading to an multiobjective optimization problem.

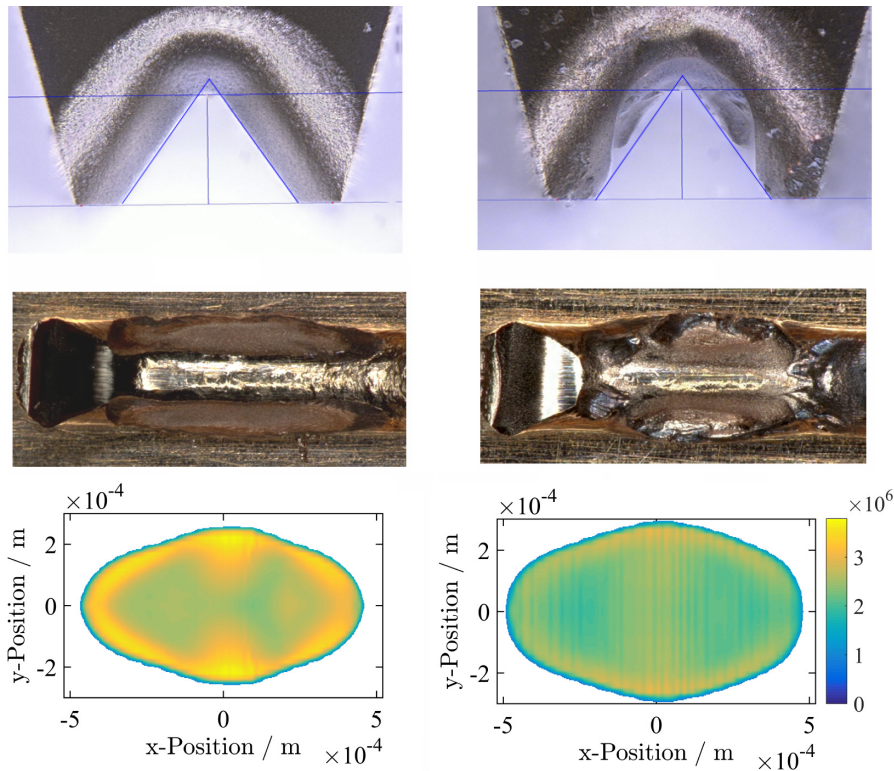


Figure 3: Wear processes in the v-groove of the wedge (top) and the influence of the worn geometry on the deformation behaviour of the wire (middle) and normal pressure distribution from finite element simulations in the interface between wire and substrate (bottom), [Unger 2017].

4 Modelling the bond formation

In the past, several approaches for modelling the bond formation in dependence of the friction energy have been reported, [Gaul et al. 2009], [Althoff et al. 2013]. In this contribution, a

differential equation system is used to simulate the bond formation, [Schemmel et al. 2018]:

$$\begin{aligned}\dot{\gamma} &= \beta P_f \quad \forall \quad \gamma < 1 \\ \dot{\gamma} &= 0 \quad \forall \quad \gamma \geq 1 \\ \dot{\tau} &= \gamma \alpha P_f \quad \forall \quad P_f \geq P_0 \\ \dot{\tau} &= 0 \quad \forall \quad P_f < P_0\end{aligned}\tag{2}$$

In **Eq. 2**, the state γ represents the cleaning state of the interface. The cleaning state can have values from 0 (initial state) up to 1 (fully cleaned). In the cleaning phase, oxide layers and other contaminations are removed from the interface. Analogous to Fleischer's law the friction power P_f (in the partial area of the interface) leads to a rising cleaning state γ due to frictional wear of oxide layers in the contact. Additionally, the real contact area increases due to deformation of asperities under the influence of ultrasound, [Bai et al. 2016]. The second state τ represents the degree of bond strength, which is influenced by the cleaning state and the frictional power P_f ; remaining oxide layers and contaminations aggravate the bond formation and an activation power P_0 is needed for a rising weld strength, [Gaul et al. 2009]. The coefficients β and α have to be determined from measurements. In [Althoff et al. 2015], the cleaning phase has been studied in experiments which can be used to derive the coefficient β , see **Figure 4**. An adapter block is used to fix 500 μm copper wires with an inelastic glue. The adapter block is excited with an oscillation amplitude $x_s = 12.1 \mu m$. A low excitation frequency of 50 Hz is used for an isolated investigation of the cleaning process without ultrasonic effects like the additional deformation of asperities with ultrasound. The results show that due to cleaning processes in the interface, the friction coefficient increases with increasing frictional energy, that has been accumulated over the oscillation time.

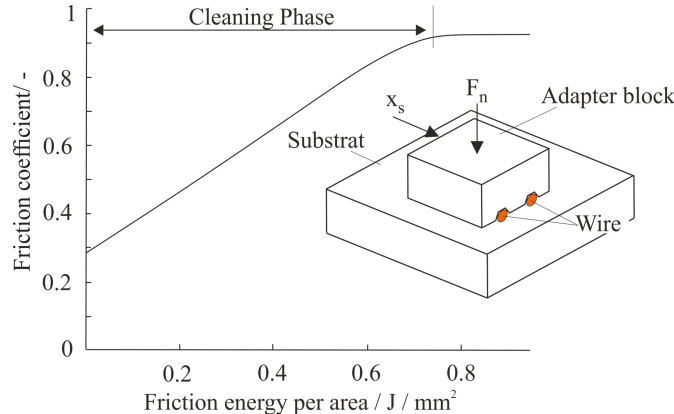


Figure 4: Experimental investigations of the friction coefficient in the cleaning phase. Two 500 μm copper wires are glued to an adapter block which is excited with an amplitude x_s and a frequency of 50 Hz, [Althoff et al. 2015]. The curve shows the approximation to multiple single measurements at different normal loads F_n in the range between 10 N and 150 N.

The simplified differential equation system in **Eq. 2** uses the frictional power P_f calculated by a frictional point contact model. The point contact model can be either applied to the whole

interface area between wire and substrate, leading to a generalized contact model or a discretized microslip model where the interface area is discretized into partial contact areas. Due to the small excitation amplitudes in the range of 1-10 μm in heavy wire bonding, typically no gross slip between wire and substrate can be seen, except in the cleaning phase. Even though no sliding between wire and substrate as a whole occurs, there is partial slip in the interface; this makes a discretized microslip model suitable for a more detailed simulation, considering micro- and macro-slip, [Hu et al. 2006], [Althoff et al. 2013], [Unger et al. 2016], [Unger 2017].

The interface area is discretized and the normal pressure distribution - which is calculated by the finite element model - is assigned to the partial areas. In **Figure 5**, the simulated distribution of the bond strength can be seen. The bond strength is directly affected by the distribution of the normal pressure, which affects the frictional power in the partial area. A typical feature of the bond strength distribution in ultrasonic wire bonding is the elliptical ring shape of areas with high bond strength which are related to areas of high frictional power during the ultrasonic excitation of the wire.

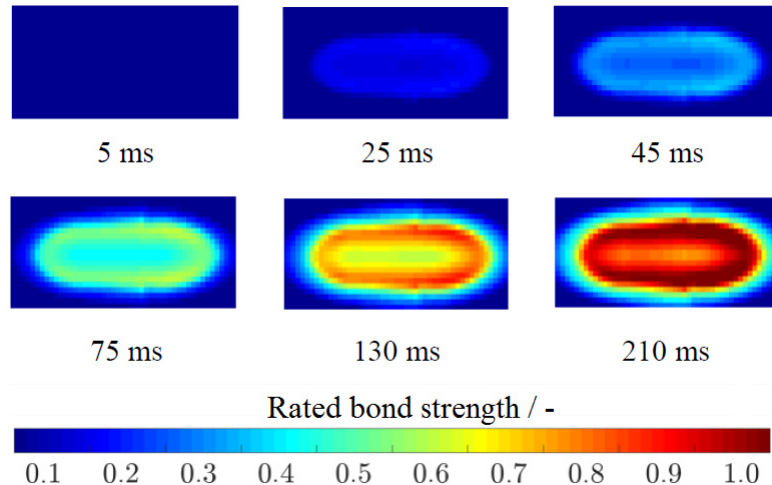


Figure 5: Simulated distribution of bond strength (rated from 0 (low) to 1 (high)) at different cut off times of the bond formation process, using the microslip friction model, [Unger et al. 2016].

5 Modelling the substrate dynamics

The substrate dynamics play an important role in ultrasonic wire bonding, especially when bonding on supple substrates. For describing the dynamical behaviour of the substrate, the mode superposition method can be used, [Hatch 2000], [Schemmel et al. 2018]. The modal matrix and eigenfrequencies as a result of a numerical modal analysis of the substrate are used to create a state-space representation:

$$\begin{aligned}\dot{\underline{x}} &= \underline{A} \underline{x} + \underline{B} \underline{u} \\ \underline{y} &= \underline{C} \underline{x}\end{aligned}\tag{3}$$

In Eq. 3, \underline{A} is the system matrix, \underline{B} is the input matrix, and \underline{C} is the output matrix. The output \underline{y} of the system is chosen by the user; in case of modelling the substrate dynamics, the displace-

ment and velocity output at the bond position are of interest. The model order of the state space system in **Eq. 3** depends on the number of modes, that are taken into account. In order to reduce the simulation time, the relevance of the states on the selected output are rated by the controllability and observability of the states with the "Hankel Singular Values" (HSV). Therefor, the gramian matrices of controllability ($\underline{\Gamma}_S$) and observability ($\underline{\Gamma}_B$) are used, [Hatch 2000]. When using the balanced transformation of the state space system from **Eq. 3**, the gramians of the balanced system are equal, $\underline{\Gamma}_S = \underline{\Gamma}_B = \text{diag}(\sigma_1, \dots, \sigma_n)$ with σ_i the HSV.

In this contribution a "Direct Copper Bonded" (DCB) plate is used as a substructure. The DCB-plate is fixed at the edge of a rubber plate and the bond position is placed at the edge of the DCB-plate. In the numerical modal analysis, different types of plate vibration modes can be seen, **Figure 6**. In the next step, the HSV are calculated to reduce the order of the state

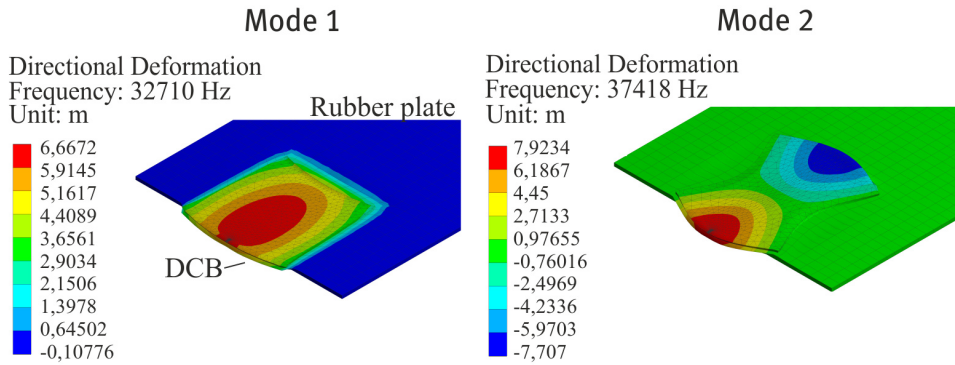


Figure 6: Results of a numerical modal analysis of the investigated substructure, consisting of a "Direct Copper Bonded" (DCB) plate, which is fixed on a rubber plate. Two representative inplane mode shapes of the DCB-plate are shown.

space system. The initial system order consists of 300 modes, leading to 600 states. In **Figure 7**, the first 40 HSV, ordered by their magnitude, are shown. For the model order reduction, states related to HSV with a small magnitude are truncated. In this example, a reduced state space system with the first 20 states and with the first 10 states was created. The frequency response of the three state space systems shows, that a very good agreement between the reduced system (20 states) and the full system (300 states) can be seen. In case of the reduced system with 10 states, less accuracy in the approximation of the full system is reached. In the following, the reduced order model with 20 states is used for numerical investigation.

With the reduced state space system of the substrate substructure a dynamical system analysis of the bond formation at two different excitation frequencies is carried out. Therefor, the whole system behaviour including the substructures of the ultrasonic transducer, the wire mass, and the substrate are used. A reduced model for the ultrasonic transducer was presented in [Unger et al. 2015]. Two different excitation frequencies of the transducer are investigated; one below the first resonance frequency of the substrate (f_1) and one above the last relevant resonance frequency (f_2). The bond duration was chosen in a way that the number of oscillations at the end of the bond process was the same for both excitation frequencies f_1 and f_2 . The sim-

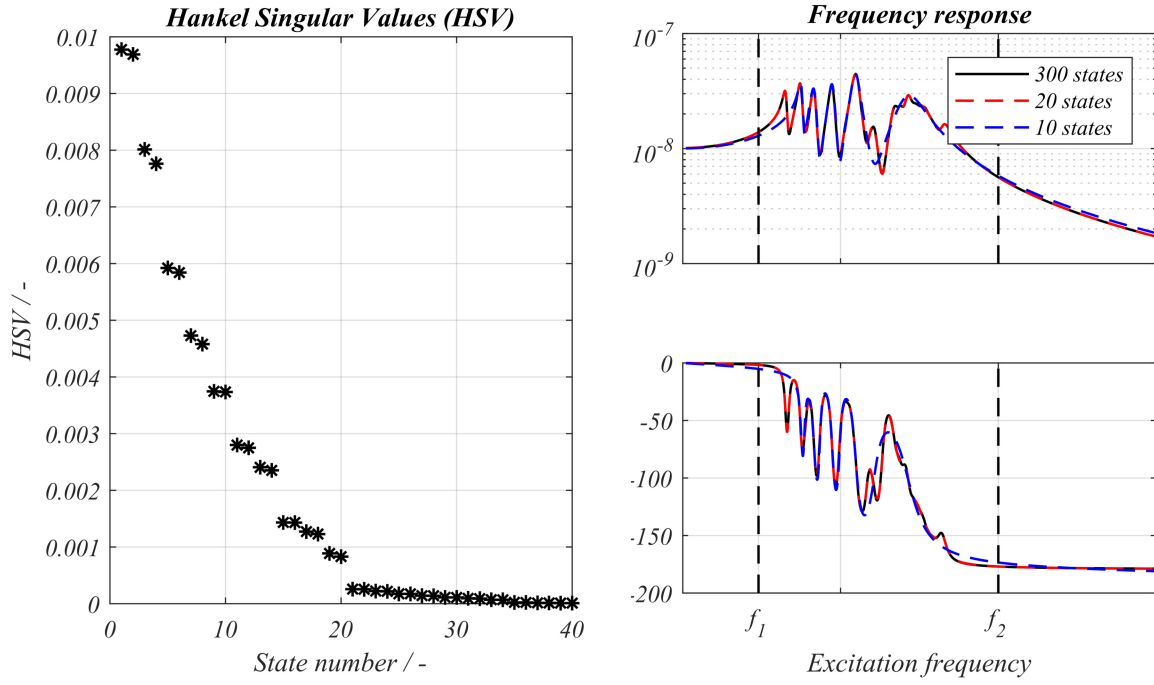


Figure 7: The first 40 "Hankel Singular Values" (HSV) of the state space system of the substrate substructure (left) and frequency response function of the full and reduced systems (right). In the frequency response, the two investigated excitation frequencies f_1 and f_2 are marked by the dashed lines.

ulated velocity amplitudes of the wire and the substrate at the bond position, the bond strength τ and the phase differences of the movement between the tool and the wire as well as between the wire and the substrate are depicted in **Figure 8**. At the excitation frequency f_2 the wire overshoots in the cleaning phase at the beginning of the bond formation and then gets bonded to the substrate while the wire amplitude decreases. In comparison, the simulation results for the excitation frequency f_1 show a two times higher substrate amplitude and a different behaviour of the wire movement; as the wire gets bonded to the substrate, the wire amplitude does not decrease significantly.

The different dynamical behaviour between the two excitation frequencies can be explained by the over-resonant excitation in case of f_2 , which can also be seen in the phase differences between tool and wire and wire and substrate, which are temporarily 180°, depending on the degree of bond strength τ . In case of bonding with f_1 , a inphase motion between tool, wire, and substrate can be seen. The dynamical behaviour has a high influence on the induced frictional power in the interface between wire and substrate; in case of f_2 a higher frictional power due to the lower substrate amplitudes and the phase difference of the motion between wire and substrate can be seen. When modelling the bond formation with the differential equation system in **Eq. 2**, the time integration of the frictional power P_f leads to a rising bond strength τ and thus, less saturation in bond formation can be seen for f_2 .

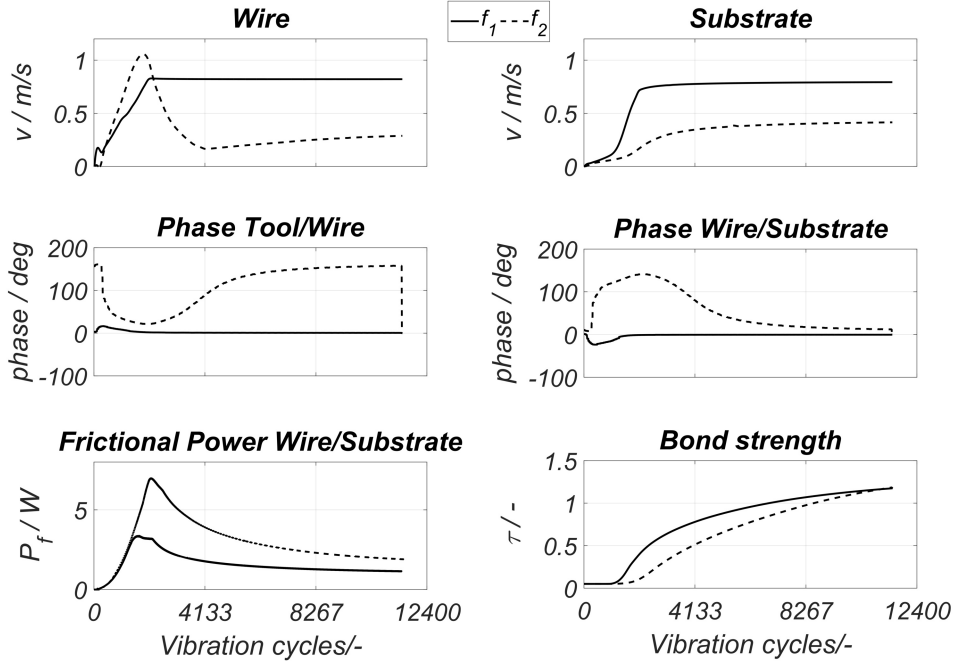


Figure 8: Simulation results: velocity amplitude of the wire and the substrate (top), phase difference between the tool and the wire as well as between the wire and the substrate (middle), frictional power in the interface and the bond strength τ (bottom), [Schemmel et al. 2018].

6 Conclusions

Modelling the bonding process under consideration of nonlinear contact behaviour and substrate dynamics is essential for a detailed insight of the bond formation behaviour. The contact between wedge and wire is crucial for the transmission of the vibration amplitude of the wedge to the wire and for the calculation of wear processes, which influence the geometry of the v-groove and the normal pressure distribution in the interface between wire and substrate. The friction contact between wire and substrate shows a time dependent behaviour, depending on the different bond phases. A differential equation system is used, to simulate the cleaning and bonding process. For modelling the dynamics of the substructure, the mode superposition method is used. A model order reduction, based on the concept of rating the relevance of the states of the system by the HSV leads to a time efficient and accurate reduced model.

A system model, consisting of models of the substructures of the transducer, wire mass, and the substrate is used to simulate the full bonding process. The simulation results at different excitation frequencies show a high influence of the substrate dynamics on the bond formation process; bonding with an excitation frequency higher than the last relevant mode leads to an over-resonant excitation with lower substrate amplitudes compared to a excitation frequency below the first resonance frequency.

Acknowledgement

Some results presented in this paper originate from a research project funded by the German Federal Ministry of Education and Research (BMBF) within the Leading-Edge Cluster Compe-

tition its OWL (intelligent technical systems OstWestfalenLippe) and managed by the Project Management Agency Karlsruhe (PTKA). The authors acknowledge the support of Hesse GmbH and Infineon Technologies AG, who were research partners in this project.

References

- Althoff, Simon, Jan Neuhaus, Tobias Hemsel, and Walter Sextro (2013). “A friction based approach for modeling wire bonding”. In: *IMAPS 2013, 46th International Symposium on Microelectronics*. Orlando (Florida), USA. DOI: 10.4071/isom-2013-TA67.
- Althoff, Simon, Andreas Unger, Walter Sextro, and Florian Eacock (2015). “Improving the cleaning process in copper wire bonding by adapting bonding parameters”. In: *2015 17th Electronics Packaging Technology Conference*, pp. 1–6. DOI: 10.1109/EPTC.2015.7412402.
- Althoff, Simon, Tobias Meyer, Andreas Unger, Walter Sextro, and Florian Eacock (2016). “Shape-Dependent Transmittable Tangential Force of Wire Bond Tools”. In: *IEEE 66th Electronic Components and Technology Conference*, pp. 2103–2110. DOI: 10.1109/ECTC.2016.234.
- Bai, Yang and Ming Yang (2016). “The influence of superimposed ultrasonic vibration on surface asperities deformation”. In: *Journal of Materials Processing Technology* 229, pp. 367 –374. ISSN: 0924-0136. DOI: <https://doi.org/10.1016/j.jmatprotec.2015.06.006>. URL: <http://www.sciencedirect.com/science/article/pii/S0924013615300170>.
- Broekelmann, M., D. Siepe, M. Hunstig, K. Guth, and M. Schnietz (2016). “Wear optimized consumables for copper wire bonding in industrial mass production”. In: *CIPS 2016; 9th International Conference on Integrated Power Electronics Systems*, pp. 1–7.
- Celnikier, Y., L. Benabou, L. Dupont, and G. Coquery (2011). “Investigation of the heel crack mechanism in Al connections for power electronics modules”. In: *Microelectronics Reliability* 51.5, pp. 965 –974. ISSN: 0026-2714. DOI: <https://doi.org/10.1016/j.microrel.2011.01.001>. URL: <http://www.sciencedirect.com/science/article/pii/S0026271411000035>.
- Chauhan, Preeti S., Anupam Choubey, ZhaoWei Zhong, and Michael G. Pecht (2014). *Copper Wire Bonding*. New York. Springer. ISBN: 978-1-4614-5760-2.
- Daud, Yusof, Margaret Lucas, and Zhihong Huang (2007). “Modelling the effects of superimposed ultrasonic vibrations on tension and compression tests of aluminium”. In: *Journal of Materials Processing Technology* 186.1, pp. 179 –190. ISSN: 0924-0136. DOI: <https://doi.org/10.1016/j.jmatprotec.2006.12.032>. URL: <http://www.sciencedirect.com/science/article/pii/S0924013606011733>.
- Eichwald, Paul, Andreas Unger, Florian Eacock, Simon Althoff, Walter Sextro, Karsten Guth, Michael Brkelmann, and Hunstig Matthias (2016). “Micro Wear Modeling in Copper Wire Wedge Bonding”. In: *IEEE CPMT Symposium Japan, 2016*.
- Eichwald, Paul, Simon Althoff, Reinhard Schemmel, Walter Sextro, Andreas Unger, Michael Brökelmann, and Matthias Hunstig (2017). “Multi-dimensional Ultrasonic Copper Bonding New Challenges for Tool Design”. In: *IMAPSource Vol. 2017, No. 1*. URL: https://doi.org/10.4071/isom-2017-WP43_071.
- Gaul, Holger, M. Schneider-Ramelow, and H. Reichl (2009). “Analysis of the friction processes in ultrasonic wedge/wedge-bonding”. In: *Microsystem Technologies* 15.5, pp. 771–

775. ISSN: 1432-1858. DOI: 10.1007/s00542-009-0811-8. URL: <https://doi.org/10.1007/s00542-009-0811-8>.
- Hatch, M.R. (2000). *Vibration Simulation Using MATLAB and ANSYS*.
- Hu, C.M., N. Guo, H. Du, W.H. Li, and M. Chen (2006). “A microslip model of the bonding process in ultrasonic wire bonders Part I: Transient response”. In: *The International Journal of Advanced Manufacturing Technology* 29.9, pp. 860–866. ISSN: 1433-3015. DOI: 10.1007/s00170-005-2587-z. URL: <https://doi.org/10.1007/s00170-005-2587-z>.
- Long, Yangyang, Jens Twiefel, and Jrg Wallaschek (2017). “A review on the mechanisms of ultrasonic wedge-wedge bonding”. In: *Journal of Materials Processing Technology* 245, pp. 241–258.
- Sbeiti, M. (2013). *Thermomechanische Beschreibung der Ausbildung einer intermetallischen Phase beim Ultraschall-Wedge/Wedge-Drahtboden im Rahmen der Theorie der materiellen Kräfte*. Schriftenreihe des Lehrstuhls für Kontinuumsmechanik und Materialtheorie der Technischen Universität Berlin. Cuvillier Verlag. ISBN: 9783954044467. URL: <https://books.google.de/books?id=leTYoAEACAAJ>.
- Schemmel, Reinhard, Simon Althoff, Michael Brökelmann, Andreas Unger, Matthias Hunstig, and Walter Sextro (2018). “Effects of different working frequencies on the joint formation in copper wire bonding”. In: *CIPS 2018 - 10th International Conference on Integrated Power Electronics Systems (CIPS 2018)*.
- Unger, A. (2017). “Modellbasierte Mehrzieloptimierung zur Herstellung von Ultraschall- Drahtbondverbindungen in Leistungshalbleitermodulen”. PhD thesis. Universität Paderborn.
- Unger, Andreas, Walter Sextro, Tobias Meyer, Paul Eichwald, Simon Althoff, Florian Eacock, Michael Brökelmann, Matthias Hunstig, and Karsten Guth (2015). “Modeling of the Stick-Slip Effect in Heavy Copper Wire Bonding to Determine and Reduce Tool Wear”. In: *2015 17th Electronics Packaging Technology Conference*. DOI: 10.1109/EPTC.2015.7412375.
- Unger, Andreas, Reinhard Schemmel, Tobias Meyer, Florian Eacock, Paul Eichwald, Simon Althoff, Walter Sextro, Michael Brökelmann, Matthias Hunstig, and Karsten Guth (2016). “Validated Simulation of the Ultrasonic Wire Bonding Process”. In: *Ultrasonics Symposium (IUS), 2016 IEEE International*. IEEE CPMT Symposium Japan, pp. 251–254.
- Xu, Tao, Todd Walker, Raymond Chen, Jason Fu, and Christoph Luechinger (2015). “Bond Tool Life Improvement for Large Copper Wire Bonding”. In: *2015 IEEE 17th Electronics Packaging and Technology Conference (EPTC)*.